

# Everything Can Be Described in Words: A Simple Unified Multi-Modal Framework with Semantic and Temporal Alignment

**Xiaowei Bi**

Northwestern University  
xiaoweibi2021@u.northwestern.edu

**Zheyuan Xu**

IEEE Member  
cx1014@uw.edu

## Abstract

While multi-modal learning has advanced significantly, current approaches often create inconsistencies in representation and reasoning of different modalities. We propose UMaT, a theoretically-grounded framework that unifies visual and auditory inputs as structured text for large language models, addressing semantic alignment, temporal synchronization, and efficient sparse information retrieval. It significantly improves state-of-the-art Long Video Question Answering accuracy (up to 13.7%, and 16.9% on long videos) via redundancy minimization and structured textual representation for unified multi-modal reasoning.

## 1 Introduction

Integrating heterogeneous modalities (vision, audio, text) remains a key AI challenge, despite progress in large-scale multi-modal models (Guo et al., 2019; Wang et al., 2022; Ye et al., 2023). However, separate encoding pathways often lead to representational issues, scalability limits, and poor transfer (Fu et al., 2021; Yang et al., 2022).

Long Video Question Answering (LVQA) highlights these challenges due to scattered information, modality alignment needs, and computational constraints. Existing LVQA methods truncate content or use resource-intensive architectures prone to semantic drift and redundancy, largely due to a lack of unified cross-modal representation.

We introduce UMaT (Unified Multi-modal as Text) with the following contributions:

- Formulation of multi-modal alignment via textual representation with optimal

information preservation and minimized redundancy.

- Novel temporal segmentation and contextual alignment for semantic coherence and efficient retrieval-augmented generation.
- Information-theoretic content deduplication adaptively filtering redundancy while preserving critical signals with provable retention.
- Significant improvement in state-of-the-art LVQA performance, particularly on long, information-sparse videos.

UMaT offers a modular and interpretable solution adaptable to various scales and domains beyond LVQA, unlike black-box methods.

## 2 Related Work

Retrieval-Augmented Generation (RAG) is increasingly used to enhance multi-modal large language models, as demonstrated by Wang et al.’s (Wang et al., 2023) proactive image questioning for visual QA, Lin and Byrne’s (Lin and Byrne, 2022) integrated differentiable dense retrieval, Lin et al.’s (Lin et al., 2023) work on adversarial visual QA, and PreFLMR’s (Lin et al., 2024) state-of-the-art knowledge-based visual QA. Video-RAG (Luo et al., 2024) applies this to video using visually-aligned text to improve visual-language models; however, these retrieval methods often treat modalities as separate streams without a unified representation.

Creating unified representations across modalities with differing dimensionality and

semantics is challenging. Cross-Modal Generalization (Xia et al., 2024) and training-free methods (Huang et al., 2024) address this, while Zhu and Li (Zhu and Li, 2023) use contrastive learning for image-text retrieval, and Video-XL (Shu et al., 2024) condenses video using Visual Summarization Tokens. However, these methods often involve complex architectures and lack theoretical grounding for optimal cross-modal information preservation.

Efficient temporal data processing benefits from segmentation and deduplication, as shown by Tirumala et al. (Tirumala et al., 2023) using pre-trained embeddings for LLM training and Liu et al.’s (Liu et al., 2023) dynamic token masking for variable-length video robustness. For finer understanding, Momentor (Qian et al., 2024) enables segment-level reasoning, SlowFast-LLaVA (Xu et al., 2024b) uses a two-stream design for spatial and temporal context, a Hierarchical Keyframe Selector (Park et al., 2024) reduces keyframes, and an iterative approach (Wang et al., 2024a) gathers relevant information; however, these temporal processing methods lack a unified framework for optimal information and efficiency balance.

Long-form video understanding faces challenges due to long temporal dependencies and sparse information (Song et al., 2025), (Liu et al., 2025), (Wang et al., 2025). LongVLM (Weng et al., 2024) addresses this by segmenting videos and using hierarchical token merging for local features. LLoVi (Zhang et al., 2024a) generates textual descriptions of short video clips via captioning. Other methods focus on specific tasks like intent reasoning (IntentQA (Li et al., 2023)), prompt robustness (PLLaVA (Xu et al., 2024a)), question-aware memory (MovieChat+ (Song et al., 2024)), and temporal localization (TimeChat (Ren et al., 2023)). However, these approaches often lack interpretability and a unified cross-modal representation.

### 3 Problem Formulation

#### 3.1 Multi-Modal Alignment Problem

Given a video  $V$  with visual content  $V_v$  and audio content  $V_a$ , we aim to create a unified representation that preserves the semantics of both modalities (visual and audio)  $\mathcal{M} = \{v, a\}$ . For each modality  $m \in \mathcal{M}$ , we have a sequence of raw inputs  $X^m = \{x_1^m, x_2^m, \dots, x_{T_m}^m\}$  where  $T_m$  is the length of the sequence for modality  $m$ . For visual content,  $x_i^v$  represents a frame or short clip, while for audio,  $x_i^a$  represents a short audio segment.

The multi-modal alignment problem can be formulated as finding mapping functions  $f_m : X^m \rightarrow \mathcal{T}$  for each modality  $m$  that transform inputs into a shared textual space  $\mathcal{T}$ , such that:

$$\begin{aligned} \min_{f_v, f_a} \quad & \mathcal{L}(f_v, f_a) \\ \text{s.t.} \quad & I(X^m; f_m(X^m)) \geq (1 - \epsilon)H(X^m), \\ & \forall m \in \mathcal{M} \end{aligned} \tag{1}$$

where  $I(\cdot; \cdot)$  represents mutual information,  $H(\cdot)$  represents entropy,  $\epsilon$  is a small constant determining allowable information loss, and  $\mathcal{L}$  is a loss function measuring semantic alignment between modalities. The formulation ensures that the textual representations preserve as much information as possible from the original modalities while staying within the textual space.

#### 3.2 Temporal Alignment and Segmentation

The temporal alignment problem involves creating aligned segments  $S = \{S_1, S_2, \dots, S_K\}$  where each segment  $S_k$  contains temporally aligned textual representations from all modalities:

$$S_k = \{(f_m(x_i^m), t_i^m) \mid t_i^m \in [t_k^{\text{start}}, t_k^{\text{end}}], m \in \mathcal{M}\} \tag{2}$$

where  $[t_k^{\text{start}}, t_k^{\text{end}}]$  defines the time interval for segment  $k$ .

### 3.3 Information-Theoretic Content Selection

Processing long videos with numerous segments can exceed language model capacity, necessitating efficient relevant segment retrieval for a given query  $q$ . We formulate this as an information-theoretic optimization problem to find a segment subset  $S_q \subset S$  that maximizes the conditional mutual information with the query response  $r$  given  $q$ , with  $\mathcal{P}(S)$  being the segment power set:

$$S_q^* = \arg \max_{S_q \in \mathcal{P}(S)} I(S_q; r | q) \quad (3)$$

s.t.  $|S_q| \leq L$

where  $L$  is the maximum number of segments that can be processed within computational constraints. This formulation aims to select segments with most information about the desired response given the query, while respecting computational constraints.

## 4 Method

### 4.1 Unified Multi-Modal Textual Representation

UMaT unifies visual and auditory inputs into text using encoders  $\phi_v$  and  $\phi_a$ .

For a video  $V$  segmented into clips  $v_i \in \mathbb{R}^{T_v \times H \times W \times 3}$ , textual captions  $c_i$  are generated by  $\phi_v(v_i)$  with a prompting strategy  $\mathcal{P}$ , which emphasizes objective scene content (composition, attributes, actions, spatial relations):

$$c_i = \phi_v(v_i, \mathcal{P})$$

Corresponding audio segments  $a_i$  are transcribed into  $t_i = \phi_a(a_i)$ , structured as  $(t_i^{\text{start}}, t_i^{\text{end}}, t_i^{\text{text}})$ .

### 4.2 Information-Preserving Temporal Alignment

To align visual captions  $\{c_i\}$  and audio transcriptions  $\{t_i\}$  temporally for coherent video representation, we segment them into fixed-length temporal segments  $S_k$ :

$$S_k = \bigcup_{i=kT_s}^{(k+1)T_s-1} \{(c_i, t_i)\}$$

where  $T_s$  is the segment size.

Information density  $\rho(S_k)$  within each segment is defined as:

$$\rho(S_k) = \frac{H(S_k)}{\sum_{i=kT_s}^{(k+1)T_s-1} |c_i| + |t_i|}$$

where  $H(S_k)$  is the entropy and  $|c_i|, |t_i|$  are lengths.

The optimal segment size  $T_s^*$  maximizes the minimum information density across all segments:

$$T_s^* = \arg \max_{T_s} \min_k \rho(S_k)$$

This balances segment length and information content.

### 4.3 Optimal Redundancy Minimization

Within each segment, redundancy is minimized while preserving critical information via constrained optimization.

Similarity between consecutive captions  $c_i$  and  $c_{i+1}$  is measured by:

$$\text{Sim}(c_i, c_{i+1}) = \frac{2 \cdot |\text{LCS}(c_i, c_{i+1})|}{|c_i| + |c_{i+1}|}$$

In which LCS denotes longest-common subsequences. Redundant content is removed based on an adaptive threshold  $\theta(c_i)$ :

$$c'_i = \begin{cases} c_i - \text{LCS}(c_{i-1}, c_i) & \text{if } \text{Sim}(c_{i-1}, c_i) > \theta(c_i) \\ c_i & \text{otherwise} \end{cases}$$

where  $\theta(c_i)$  adapts to caption information content:

$$\theta(c_i) = \alpha + \beta \cdot \frac{H(c_i)}{|c_i|}$$

$\alpha$  and  $\beta$  are hyperparameters.

**Theorem 1.** Given captions  $\{c_i\}$  and processed  $\{c'_i\}$  with adaptive threshold  $\theta(c_i) < 1 - \frac{H_{\text{unique}}(c_i)}{H(c_i)}$ , the processed captions preserve at least  $(1 - \epsilon)$  of the unique information.

*Proof.* Unique information  $H_{\text{unique}}(c_i) = H(c_i) - I(c_i; c_{i-1})$ . Redundancy removal eliminates  $I(c_i; c_{i-1})$ . The threshold ensures preserved information is at least  $(1 - \epsilon)H_{\text{unique}}(c_i)$ .  $\square$

This guarantees critical information preservation during efficient content reduction.

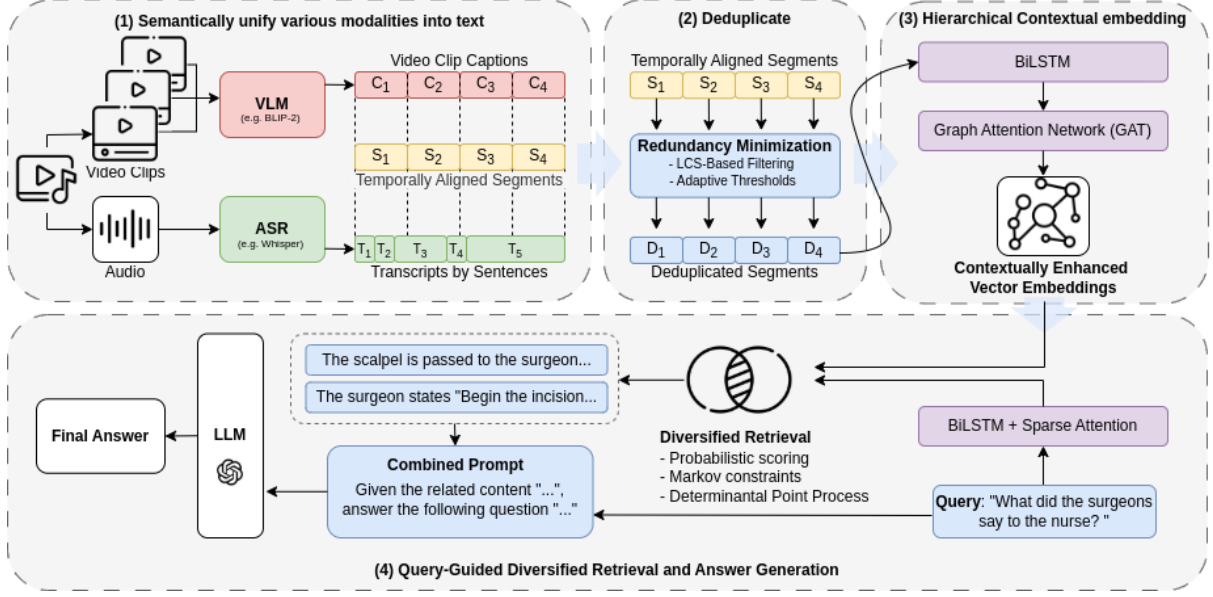


Figure 1: Flowchart showing UMaT framework: Raw video undergoes parallel processing via a VLM (visual) and ASR (audio). Resulting text is temporally aligned and fused into segments. A hierarchical contextual embedding engine creates high-dimensional vectors preserving temporal and semantic relationships. During inference, probabilistic diversified retrieval selects relevant segments for an LLM prompt.

#### 4.4 Retrieval-Augmented Generation with Dense Embeddings

For efficient query-based video segment retrieval, we use a context-aware hierarchical embedding with probabilistic selection, addressing semantic alignment, contextual coherence, and information diversity.

##### 4.4.1 Hierarchical Contextual Embedding

Let  $\mathcal{S} = \{S'_1, S'_2, \dots, S'_K\}$  be the set of all processed segments. Each segment  $S'_k$  consists of a sequence of textual elements  $S'_k = \{w_1^k, w_2^k, \dots, w_{n_k}^k\}$  representing words or tokens from both visual captions and audio transcriptions. We first employ a hierarchical embedding approach that captures both local and global semantic structure:

$$\mathbf{h}_i^k = \text{BiLSTM}(w_i^k, \mathbf{h}_{i-1}^k), \quad i \in \{1, 2, \dots, n_k\} \quad (4)$$

$$\mathbf{a}_i^k = \frac{\exp(\mathbf{v}^T \tanh(\mathbf{W}\mathbf{h}_i^k + \mathbf{b}))}{\sum_{j=1}^{n_k} \exp(\mathbf{v}^T \tanh(\mathbf{W}\mathbf{h}_j^k + \mathbf{b}))} \quad (5)$$

$$\mathbf{e}_k^{\text{local}} = \sum_{i=1}^{n_k} \mathbf{a}_i^k \mathbf{h}_i^k \quad (6)$$

where  $\mathbf{h}_i^k$  is the hidden state of the BiLSTM for token  $i$  in segment  $k$ ,  $\mathbf{a}_i^k$  is the attention weight, and  $\mathbf{e}_k^{\text{local}}$  is the local segment embedding.

To capture global contextual information and temporal relationships, we introduce a graph-based contextual enhancement:

$$\mathcal{G} = (\mathcal{V}, \mathcal{E}, \mathbf{A}) \quad (7)$$

where  $\mathcal{V} = \{v_1, v_2, \dots, v_K\}$  is the set of vertices corresponding to segments,  $\mathcal{E}$  is the set of edges representing temporal proximity and semantic similarity, and  $\mathbf{A} \in \mathbb{R}^{K \times K}$  is the adjacency matrix with elements:

$$A_{i,j} = \alpha \cdot \exp(-\beta|i-j|) + (1-\alpha) \cdot \cos(\mathbf{e}_i^{\text{local}}, \mathbf{e}_j^{\text{local}}) \quad (8)$$

if  $|i-j| \leq \delta$  or  $\cos(\mathbf{e}_i^{\text{local}}, \mathbf{e}_j^{\text{local}}) \geq \tau$   
and 0 otherwise

where  $\alpha, \beta, \delta, \tau$  are hyperparameters controlling the balance between temporal and semantic relationships.

We then apply a graph attention network (GAT) to obtain contextually enhanced embeddings:

$$\mathbf{e}_k^{(0)} = \mathbf{e}_k^{\text{local}} \quad (9)$$

$$\mathbf{e}_k^{(l+1)} = \sigma \left( \sum_{j \in \mathcal{N}(k)} \gamma_{kj}^{(l)} \mathbf{W}^{(l)} \mathbf{e}_j^{(l)} \right) \quad (10)$$

$$\text{LeakyReLU}(j) = \text{LeakyReLU} \left( \mathbf{a}^{(l)T} [\mathbf{W}^{(l)} \mathbf{e}_k^{(l)} \parallel \mathbf{W}^{(l)} \mathbf{e}_j^{(l)}] \right) \quad (11)$$

$$\gamma_{kj}^{(l)} = \frac{\exp(\text{LeakyReLU}(j))}{\sum_{m \in \mathcal{N}(k)} \exp(\text{LeakyReLU}(m))} \quad (12)$$

where  $\mathcal{N}(k)$  is the neighborhood of vertex  $k$  in graph  $\mathcal{G}$ ,  $\gamma_{kj}^{(l)}$  is the attention coefficient at layer  $l$ ,  $\mathbf{W}^{(l)}$  is a learnable weight matrix,  $\mathbf{a}^{(l)}$  is a learnable attention vector, and  $\parallel$  represents concatenation. The final embedding for segment  $k$  is:

$$\mathbf{e}_k = \mathbf{e}_k^{(L)} + \lambda \mathbf{e}_k^{\text{local}} \quad (13)$$

where  $L$  is the number of GAT layers and  $\lambda$  is a residual connection weight.

#### 4.4.2 Query Representation with Sparse Attention

For the query  $q = \{q_1, q_2, \dots, q_m\}$ , we employ a sparse attention mechanism that focuses on the most discriminative terms:

$$\mathbf{h}_i^q = \text{BiLSTM}(q_i, \mathbf{h}_{i-1}^q), \quad i \in \{1, 2, \dots, m\} \quad (14)$$

$$\tilde{\mathbf{a}}_i^q = \mathbf{v}_q^T \tanh(\mathbf{W}_q \mathbf{h}_i^q + \mathbf{b}_q) \quad (15)$$

$$\mathbf{a}_i^q = \frac{\exp(\tilde{\mathbf{a}}_i^q) \cdot \mathbb{1}[\tilde{\mathbf{a}}_i^q > \theta_q]}{\sum_{j=1}^m \exp(\tilde{\mathbf{a}}_j^q) \cdot \mathbb{1}[\tilde{\mathbf{a}}_j^q > \theta_q]} \quad (16)$$

$$\mathbf{e}_q = \sum_{i=1}^m \mathbf{a}_i^q \mathbf{h}_i^q \quad (17)$$

where  $\theta_q$  is a threshold parameter for sparse attention, focusing only on the most relevant terms in the query.

#### 4.4.3 Probabilistic Diversified Retrieval

Instead of a simple similarity-based retrieval, we formulate the segment selection as a probabilistic optimization problem that balances relevance, diversity, and coverage:

$$P(S'_k | q) = \frac{\exp(\phi(S'_k, q)/\rho)}{\sum_{j=1}^K \exp(\phi(S'_j, q)/\rho)} \quad (18)$$

where  $\phi(S'_k, q)$  is a relevance function and  $\rho$  is a temperature parameter. We define the relevance function as:

$$\phi(S'_k, q) = \cos(\mathbf{e}_k, \mathbf{e}_q) \cdot (1 + \eta \cdot \text{Novelty}(S'_k, \mathcal{S}_q)) \quad (19)$$

where  $\cos(\cdot, \cdot)$  is the cosine similarity,  $\mathcal{S}_q$  is the set of already selected segments, and  $\text{Novelty}(S'_k, \mathcal{S}_q)$  measures the information gain of adding segment  $S'_k$  to the already selected segments:

$$\text{Novelty}(S'_k, \mathcal{S}_q) = 1 - \max_{S'_j \in \mathcal{S}_q} \cos(\mathbf{e}_k, \mathbf{e}_j) \quad (20)$$

We select segments sequentially according to a determinantal point process (DPP) that enforces diversity:

$$\mathcal{S}_q = \arg \max_{\mathcal{S} \subset \mathcal{S}, |\mathcal{S}|=M} \det(\mathbf{L}_{\mathcal{S}}) \quad (21)$$

where  $\mathbf{L}_{\mathcal{S}}$  is a positive semidefinite kernel matrix with elements:

$$L_{ij} = P(S'_i | q) \cdot P(S'_j | q) \cdot (1 - \omega \cos(\mathbf{e}_i, \mathbf{e}_j)) \quad (22)$$

where  $\omega$  is a diversity parameter.

To further enhance temporal coherence, we introduce a Markovian constraint that encourages the selection of temporally adjacent segments when beneficial:

$$P(S'_k | S'_{k-1}, q) = (1 - \mu) P(S'_k | q) + \mu \cdot \mathbb{1}[|k - (k-1)| = 1] \cdot \cos(\mathbf{e}_k, \mathbf{e}_q) \quad (23)$$

where  $\mu$  is a parameter controlling the strength of the Markovian constraint.

The final retrieval objective integrates all these considerations into a unified optimization framework:

$$\begin{aligned} \mathcal{S}_q^* = \arg \max_{\mathcal{S} \subset \mathcal{S}, |\mathcal{S}|=M} & \sum_{S'_k \in \mathcal{S}} P(S'_k | q) + \\ & \nu \det(\mathbf{L}_{\mathcal{S}}) + \xi \sum_{i=1}^{|\mathcal{S}|-1} P(S'_{i+1} | S'_i, q) \end{aligned} \quad (24)$$

$$\text{s.t. } \text{KL}(P(\mathcal{S}) \| P(\mathcal{S} | q)) \leq \epsilon$$

where  $\nu$  and  $\xi$  are weights, and the KL-divergence constraint prevents overfitting by limiting deviation from the prior. This retrieval formulation allows UMaT to select a contextually coherent, diverse, and relevant segment set, maximizing information value for query answering while respecting semantic and temporal video structure.

## 5 Experiments

### 5.1 Experimental Setup

#### 5.1.1 Dataset

We evaluate UMaT on Video-MME (Fu et al., 2024), a comprehensive benchmark for long video question answering. Video-MME contains 900 videos spanning six domains including Knowledge, Film & Television, etc. ranging from 11 seconds to 1 hour, making it an ideal testbed for evaluating long-form video understanding.

#### 5.1.2 Baseline Models

We compare UMaT against three state-of-the-art video-language models:

- **LLaVA-NeXT-Video** (Liu et al., 2024): A vision-language model extended for video processing, with frame-level alignment.
- **LongVA** (Zhang et al., 2024b): A specialized model for long context understanding in videos.
- **Long-LLaVA** (Wang et al., 2024b): An extension of LLaVA optimized for processing lengthy visual inputs.

We integrate UMaT with each of these models to assess its ability to enhance existing architectures through unified textual representation and efficient retrieval.

#### 5.1.3 Implementation Details

We use fine-tuned BLIP-2 (visual captioning) and Whisper-large-v3 (ASR). Optimized hyperparameters include segment size  $T_s = 30s$ , redundancy minimizing parameters  $\alpha = 0.6, \beta = 0.2$ , hierarchical embedding with  $L = 2$  GAT layers, graph enhancement  $\alpha = 0.7, \beta = 0.2, \delta = 5, \tau = 0.8$ , sparse attention

Table 1: Performance on Video-MME benchmark across various video durations. The UMaT framework consistently improves performance across all models, with significant gains for long videos.

Model	#Params	Video Duration			Overall
		Short	Medium	Long	
LLaVA-NeXT-Video	7B	50.2	44.3	38.6	44.4
LLaVA-NeXT-Video + UMaT	7B	60.2	51.2	49.2	53.5 (+9.1)
LongVA	7B	59.2	50.3	45.0	51.5
LongVA + UMaT	7B	68.5	63.1	58.3	63.3 (+11.8)
Long-LLaVA	7B	59.5	52.0	45.3	52.2
Long-LLaVA + UMaT	7B	70.3	65.1	62.2	65.9 (+13.7)

$\theta_q = 0.6$ , and diversification  $\eta = 0.5, \omega = 0.8, \mu = 0.4, \nu = 0.6, \xi = 0.3$ . These values were empirically determined via ablation studies. Experiments were on 4 NVIDIA A100 GPUs, with processing times around 8 seconds per minute for short videos and roughly linear scaling for longer ones.

### 5.2 Main Results

Table 1 compares baseline and UMaT-enhanced model performance across video durations, revealing:

- UMaT consistently improves accuracy (9.1% to 13.7% overall).
- Gains are highest for long videos (up to 16.9)
- Substantial improvements are also seen for short videos (up to 10.8)

These results validate our hypothesis that unified textual representation enhances multi-modal reasoning, especially for long, information-sparse content.

### 5.3 Ablation Studies

To better understand the contribution of each component in our framework, we conduct a series of ablation studies.

#### 5.3.1 Impact of Segment Size

Figure 2 illustrates the effect of segment size on QA accuracy for UMaT-enhanced models, showing an inverted U-shape with peak performance around 30 seconds. This indicates:

- Short segments (10-20s) lack sufficient context.

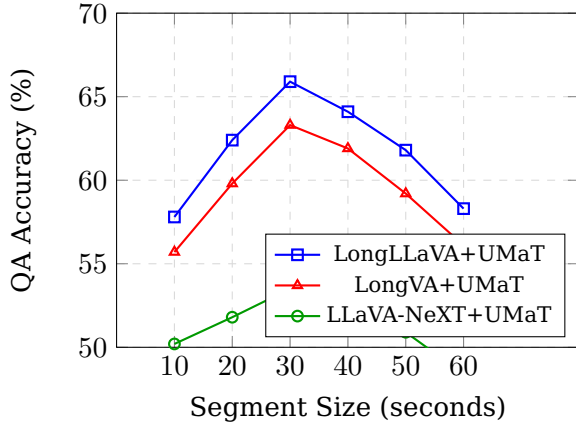


Figure 2: Impact of segment size on QA accuracy. The optimal segment size appears to be around 30 seconds, balancing context preservation and redundancy minimization.

- Long segments (50-60s) introduce noise and redundancy.
- The optimal 30-second size balances context and redundancy, consistent with information density optimization.

### 5.3.2 Contribution of Individual Components

Table 2 shows the impact of removing UMaT components on Long-LLaVA performance:

- -8.2% without ASR (critical for speech-heavy videos).
- -7.3% without graph-based contextual enhancement (importance of global context).
- -5.8% without probabilistic diversified retrieval (value of semantic diversity).
- -6.4% with simple cosine similarity (importance of our retrieval formulation).
- -4.2% without redundancy minimization (benefit of efficient representation).

These results confirm the substantial contribution of each UMaT component.

### 5.3.3 Analysis of Retrieval Effectiveness

Table 3 compares retrieval methods with Long-LLaVA + UMaT to evaluate our mechanism:

Table 2: Ablation study on Long-LLaVA + UMaT, showing the importance of each component. Results are reported on the Video-MME benchmark.

Configuration	Accuracy (%)
Full UMaT framework	65.9
No ASR	57.7 (-8.2)
No graph-based enhancement	58.6 (-7.3)
Simple cosine similarity	59.5 (-6.4)
No diversified retrieval	60.1 (-5.8)
No redundancy minimization	61.7 (-4.2)

Table 3: Comparison of different retrieval methods on Long-LLaVA + UMaT.

Retrieval Method	Accuracy (%)
Probabilistic DPP (ours)	65.9
Greedy selection	61.3 (-4.6)
Temporal	57.8 (-8.1)
Random	50.4 (-15.5)

- Probabilistic DPP (Ours): Full probabilistic retrieval with DPP.
- Greedy: Iterative selection by relevance.
- Temporal: Selection based on temporal proximity.
- Random: Random segment selection.

Our probabilistic DPP significantly outperforms other methods, highlighting the importance of relevance-diversity balance for effective QA.

## 6 Theoretical Analysis

We now provide a deeper theoretical analysis of UMaT’s information-theoretic properties, focusing on the optimality of our retrieval approach.

### 6.1 Information-Theoretic Bounds on Retrieval Optimality

UMaT’s effectiveness relies on relevant segment retrieval, formalized as submodular maximization.  $I(S_q; r | q)$ , the conditional

mutual information between retrieved segments  $S_q$  and response  $r$  given query  $q$ , is submodular.

**Theorem 2** (Near-Optimal Retrieval). *Let  $S_q^*$  be the optimal  $K$  segments maximizing  $I(S_q; r | q)$ , and  $S_q^G$  be the greedy retrieval result. Then:*

$$I(S_q^G; r | q) \geq (1 - 1/e) \cdot I(S_q^*; r | q)$$

*Proof.* Greedy maximization of a submodular function yields a  $(1 - 1/e)$  approximation. Since conditional mutual information is submodular, our greedy retrieval achieves at least  $(1 - 1/e) \approx 63\%$  of the optimal value.  $\square$

This ensures near-optimal information retrieval, even for complex queries.

## 6.2 Deduplication Efficiency Analysis

Our redundancy minimization aims for content reduction while preserving critical information, which we analyze by compression ratio and information retention.

**Theorem 3.** *Let  $C$  and  $C'$  be original and deduplicated content, with compression ratio  $\kappa = |C'|/|C|$  and information retention ratio  $\iota = I(C'; r | q)/I(C; r | q)$ . Then:*

$$\kappa + \iota \geq 1 + \frac{\min_i H_{\text{unique}}(c_i)/H(c_i)}{1 - \min_i H_{\text{unique}}(c_i)/H(c_i)}$$

where  $H_{\text{unique}}(c_i)/H(c_i)$  is the unique information fraction.

*Proof.* (Sketch) Adaptive thresholding removes content based on redundancy relative to information content, establishing a trade-off between removal and preservation, leading to the bound.  $\square$

## 7 Conclusion

In conclusion, UMaT, a unified framework transforming visual and auditory inputs into structured text for large language models, confirms language as a universal interface for effective multi-modal reasoning. Its modularity, interpretability, and efficiency suit real-world, long-form multi-modal applications. Future work includes extension to more modalities (e.g., tactile, thermal) and

domains (robotics, healthcare, science), as well as exploring theoretical links to information bottleneck theory and balancing information preservation with efficiency.

## 8 Limitations

The UMaT framework for LVQA, while effective, is limited by its reliance on the performance of upstream VLMs (BLIP-2) and ASR models (Whisper-large-v3), which can introduce their own inaccuracies and biases. Furthermore, the conversion of rich visual and auditory data into a unified textual representation creates a potential risk of losing subtle details despite efforts for optimal information preservation. Although UMaT aims for efficiency, particularly with its sparse information retrieval, the multi-stage processing involving VLMs, ASR, hierarchical embeddings (BiLSTM, GAT), and probabilistic retrieval mechanisms (DPP) can still be computationally intensive, especially for extremely long videos or in resource-constrained environments, which renders it less feasible for real-time tasks. However, we believe with the scaling of computational power, it will be less of an issue in the future.

## References

- Chaoyou Fu, Yuhan Dai, Yondong Luo, Lei Li, Shuhuai Ren, Renrui Zhang, Zihan Wang, Chenyu Zhou, Yunhang Shen, Mengdan Zhang, et al. 2024. Videomme: The first-ever comprehensive evaluation benchmark of multi-modal llms in video analysis. *arXiv preprint arXiv:2405.21075*.
- Tsu-Jui Fu, Linjie Li, Zhe Gan, Kevin Lin, William Yang Wang, Lijuan Wang, and Zicheng Liu. 2021. [Violet : End-to-end video-language transformers with masked visual-token modeling](#). *ArXiv*, abs/2111.12681.
- Daya Guo, Jiangshui Hong, Binli Luo, Qirui Yan, and Zhangming Niu. 2019. [Multi-modal representation learning for short video understanding and recommendation](#). *2019 IEEE International Conference on Multimedia & Expo Workshops (ICMEW)*, pages 687–690.
- Hai Huang, Yan Xia, Shengpeng Ji, Shulei Wang, Hanting Wang, Jieming Zhu, Zhenhua Dong, and Zhou Zhao. 2024. [Unlocking the potential of multimodal unified discrete representation through training-free codebook optimization and hierarchical alignment](#). *ArXiv*, abs/2403.05168.

- Jiapeng Li, Ping Wei, Wenjuan Han, and Lifeng Fan. 2023. [Intentqa: Context-aware video intent reasoning](#). In *2023 IEEE/CVF International Conference on Computer Vision (ICCV)*, pages 11929–11940.
- Weizhe Lin and Bill Byrne. 2022. [Retrieval augmented visual question answering with outside knowledge](#). In *Proceedings of the 2022 Conference on Empirical Methods in Natural Language Processing*, pages 11238–11254, Abu Dhabi, United Arab Emirates. Association for Computational Linguistics.
- Weizhe Lin, Jingbiao Mei, Jinghong Chen, and Bill Byrne. 2024. [PreFLMR: Scaling up fine-grained late-interaction multi-modal retrievers](#). In *Proceedings of the 62nd Annual Meeting of the Association for Computational Linguistics (Volume 1: Long Papers)*, pages 5294–5316, Bangkok, Thailand. Association for Computational Linguistics.
- Weizhe Lin, Zhilin Wang, and Bill Byrne. 2023. [FVQA 2.0: Introducing adversarial samples into fact-based visual question answering](#). In *Findings of the Association for Computational Linguistics: EACL 2023*, pages 149–157, Dubrovnik, Croatia. Association for Computational Linguistics.
- Haotian Liu, Chunyuan Li, Yuheng Li, Bo Li, Yuanhan Zhang, Sheng Shen, and Yong Jae Lee. 2024. [Llava-next: Improved reasoning, ocr, and world knowledge](#).
- Ruyang Liu, Chen Li, Haoran Tang, Yixiao Ge, Ying Shan, and Ge Li. 2023. [St-llm: Large language models are effective temporal learners](#). <https://arxiv.org/abs/2404.00308>.
- Yunbo Liu, Xukui Qin, Yifan Gao, Xiang Li, and Chengwei Feng. 2025. [Setransformer: A hybrid attention-based architecture for robust human activity recognition](#). *Preprint*, arXiv:2505.19369.
- Yongdong Luo, Xiawu Zheng, Xiao Yang, Guilin Li, Haojia Lin, Jinfang Huang, Jiayi Ji, Fei Chao, Jiebo Luo, and Rongrong Ji. 2024. [Video-rag: Visually-aligned retrieval-augmented long video comprehension](#). *Preprint*, arXiv:2411.13093.
- Jong Sung Park, Kanchana Ranasinghe, Kumara Kahatapitiya, Wonjeong Ryoo, Donghyun Kim, and Michael S. Ryoo. 2024. [Too many frames, not all useful: Efficient strategies for long-form video qa](#). *ArXiv*, abs/2406.09396.
- Long Qian, Juncheng Li, Yu Wu, Yaobo Ye, Hao Fei, Tat-Seng Chua, Yueting Zhuang, and Siliang Tang. 2024. [Momentor: advancing video large language model with fine-grained temporal reasoning](#). In *Proceedings of the 41st International Conference on Machine Learning, ICML’24*. JMLR.org.
- Shuhuai Ren, Linli Yao, Shicheng Li, Xu Sun, and Lu Hou. 2023. [Timechat: A time-sensitive multi-modal large language model for long video understanding](#). *Preprint*, arXiv:2312.02051.
- Yan Shu, Peitian Zhang, Zheng Liu, Minghao Qin, Junjie Zhou, Tiejun Huang, and Bo Zhao. 2024. [Video-xl: Extra-long vision language model for hour-scale video understanding](#). *ArXiv*, abs/2409.14485.
- Enxin Song, Wenhao Chai, Weili Xu, Jianwen Xie, Yuxuan Liu, and Gaoang Wang. 2025. [Video-mmlu: A massive multi-discipline lecture understanding benchmark](#). *arXiv preprint arXiv:2504.14693*.
- Enxin Song, Wenhao Chai, Tian Ye, Jenq-Neng Hwang, Xi Li, and Gaoang Wang. 2024. [Moviechat+: Question-aware sparse memory for long video question answering](#). *Preprint*, arXiv:2404.17176.
- Kushal Tirumala, Daniel Simig, Armen Aghajanyan, and Ari S. Morcos. 2023. [D4: improving llm pre-training via document de-duplication and diversification](#). In *Proceedings of the 37th International Conference on Neural Information Processing Systems, NIPS ’23*, Red Hook, NY, USA. Curran Associates Inc.
- Chao Wang, Chuanhao Nie, and Yunbo Liu. 2025. [Evaluating supervised learning models for fraud detection: A comparative study of classical and deep architectures on imbalanced transaction data](#). *Preprint*, arXiv:2505.22521.
- Xiaohan Wang, Yuhui Zhang, Orr Zohar, and Serena Yeung-Levy. 2024a. [Videoagent: Long-form video understanding with large language model as agent](#). In *Computer Vision – ECCV 2024: 18th European Conference, Milan, Italy, September 29–October 4, 2024, Proceedings, Part LXXX*, page 58–76, Berlin, Heidelberg. Springer-Verlag.
- Xidong Wang, Dingjie Song, Shunian Chen, Chen Zhang, and Benyou Wang. 2024b. [Longllava: Scaling multi-modal llms to 1000 images efficiently via a hybrid architecture](#). *ArXiv*.
- Yi Wang, Kunchang Li, Yizhuo Li, Yanan He, Bingkun Huang, Zhiyu Zhao, Hongjie Zhang, Jilan Xu, Yi Liu, Zun Wang, Sen Xing, Guo Chen, Juntong Pan, Jiashuo Yu, Yali Wang, Limin Wang, and Yu Qiao. 2022. [Internvideo: General video foundation models via generative and discriminative learning](#). *ArXiv*, abs/2212.03191.
- Ziyue Wang, Chi Chen, Peng Li, and Yang Liu. 2023. [Filling the image information gap for vqa: Prompting large language models to proactively ask questions](#). *Preprint*, arXiv:2311.11598.
- Yuetian Weng, Mingfei Han, Haoyu He, Xiaojun Chang, and Bohan Zhuang. 2024. [Longvlm: Efficient long video understanding via large language models](#). In *Computer Vision – ECCV 2024: 18th European Conference, Milan, Italy, September 29–October 4, 2024, Proceedings, Part XXXIII*, page 453–470, Berlin, Heidelberg. Springer-Verlag.
- Yan Xia, Hai Huang, Jieming Zhu, and Zhou Zhao. 2024. [Achieving cross modal generalization with multimodal unified representation](#). *Advances in Neural Information Processing Systems*, 36.
- Lin Xu, Yilin Zhao, Daquan Zhou, Zhijie Lin, See Kiong Ng, and Jiashi Feng. 2024a. [Pllava: Parameter-free llava extension from images to videos for video dense captioning](#). *Preprint*, arXiv:2404.16994.
- Mingze Xu, Mingfei Gao, Zhe Gan, Hong-You Chen, Zhengfeng Lai, Haiming Gang, Kai Kang, and Afshin Dehghan. 2024b. [Slowfast-llava: A strong training-free baseline for video large language models](#). *ArXiv*, abs/2407.15841.

- Antoine Yang, Antoine Miech, Josef Sivic, Ivan Laptev, and Cordelia Schmid. 2022. Zero-shot video question answering via frozen bidirectional language models. In *Proceedings of the 36th International Conference on Neural Information Processing Systems, NIPS '22*, Red Hook, NY, USA. Curran Associates Inc.
- Qinghao Ye, Haiyang Xu, Guohai Xu, Jiabo Ye, Ming Yan, Yi Zhou, Junyan Wang, Anwen Hu, Pengcheng Shi, Yaya Shi, Chenliang Li, Yuanhong Xu, Hehong Chen, Junfeng Tian, Qiang Qi, Ji Zhang, and Feiyan Huang. 2023. [mplug-owl: Modularization empowers large language models with multimodality](#). *ArXiv*, abs/2304.14178.
- Ce Zhang, Taixi Lu, Md Mohaiminul Islam, Ziyang Wang, Shoubin Yu, Mohit Bansal, and Gedas Bertasius. 2024a. [A simple LLM framework for long-range video question-answering](#). In *Proceedings of the 2024 Conference on Empirical Methods in Natural Language Processing*, pages 21715–21737, Miami, Florida, USA. Association for Computational Linguistics.
- Peiyuan Zhang, Kaichen Zhang, Bo Li, Guangtao Zeng, Jingkang Yang, Yuanhan Zhang, Ziyue Wang, Hao-ran Tan, Chunyuan Li, and Ziwei Liu. 2024b. [Long context transfer from language to vision](#). *ArXiv*, abs/2406.16852.
- Yi Zhu and Xiu Li. 2023. [Iterative uni-modal and cross-modal clustered contrastive learning for image-text retrieval](#). *2023 International Conference on Pattern Recognition, Machine Vision and Intelligent Algorithms (PRMVIA)*, pages 15–23.